# FINAL TECHNICAL REPORT
## Effect of Manufacturing-Induced Defects on Reliability of Composite Wind Turbine Blades

## U.S. Department of Energy
## Award No. DE-EE0001374 ARRA Funding

## Executive Summary

## UML Report # S51900000011598

Lead Organization:
University of Massachusetts Lowell
Julie Chen, Christopher Niezrecki, James Sherwood, and Peter Avitabile
*Advanced Composite Materials and Textile Research Laboratory*
*Structural Dynamics and Acoustics Systems Laboratory*
Lowell, Massachusetts

Partner Organizations:
Mark Rumsey, Sandia National Laboratory, Albuquerque, New Mexico
Scott Hughes, National Renewable Energy Laboratory, Golden, Colorado
Stephen Nolet, TPI Composites, Warren, RI

Date: 31 August 2012

## Executive Summary

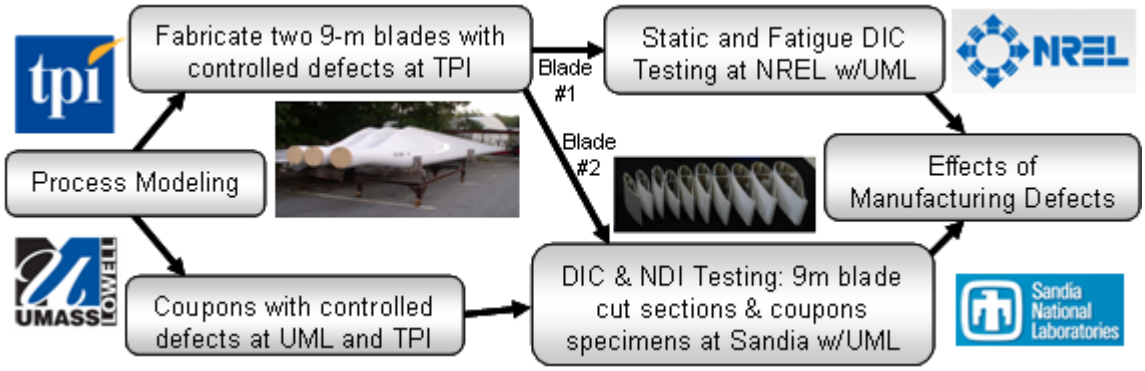


In support of DOE's efforts on developing "affordable, reliable domestic wind power", this ARRA project brought together a strong, complementary team from academia (University of Massachusetts Lowell), two DOE laboratories (NREL and Sandia), and a major wind turbine blade manufacturer (TPI) to address one of the key issues affecting wind power cost and reliability – manufacturing-induced defects in the blades. The complexity of this problem required the assembled team's expertise in materials – specifically textile and composite structures – finite element modeling, composites manufacturing, mechanical characterization, structural dynamics, nondestructive inspection (NDI) and structural health monitoring (SHM), sensors, and wind turbine blade testing.

The focus of this project was a defect referred to as a "wave defect", wrinkle, or out-of-plane buckle. The wave defect has been recognized by many in the wind industry as a defect that is difficult to prevent in the manufacturing process, difficult to detect (versus a poor bond or dry section), and highly likely to cause unexpected failure. As a result, design knockdowns (high safety factors or penalties on failure values) are overly conservative to account for such defects and even minor defects that are discovered after manufacturing can result in a blade being discarded. Both approaches lead to a significant decrease in the economic competitiveness of wind turbines. The team's goal was to address this problem by integrating efforts to:

(1) develop a model using commercially-available software to help designers identify combinations of fabric structure, blade geometry, and process conditions that are likely to lead to wave defect formation, as well as the

defect's impact on strains in the blade under load, and thus informing effective design choices;

(2) understand what wave defect geometries (e.g., aspect ratio and amplitude) and locations (both within the skin thickness and along the blade length) were most detrimental to compressive and fatigue failure, and thus should be the focus of both manufacturing approaches and inspection techniques; and

(3) further develop digital image correlation (DIC) as an effective, full-field strain and displacement measurement technique and understand its applicability for detection of wave defects and for structural health monitoring (SHM).

The project revolved around three, 9-meter, CX-100 wind turbine blades and a series of representative coupons, all fabricated at TPI. Two of the blades were fabricated specifically for this project, while the third was a blade fabricated utilizing the same layup schedule for Los Alamos National Laboratory (LANL) for another project. The key difference between the blades was that the LANL blade contained no known defects, while the "UMass Lowell" blades had wave defects of controlled geometry inserted at specified locations along the blade. Similarly, compression and fatigue coupons with and without defects of controlled aspect ratio and height were fabricated.

The LANL defect-free blade and one UMass Lowell defect blade were tested at NREL using a schedule of cycles at increasing load level until failure was detected. DIC was used as a SHM technique, along with several other methods, including acoustic emission, fiber optic strain sensors, foil strain gages, and PZT sensors for comparison and validation. The second UMass Lowell blade was cut into subcomponents and tested at Sandia.

The key outcomes from this project are:

(a) A combination of fabric-characterization tests to define material properties and a user-defined material model comprised of a beam and shell system can be used with ABAQUS and other commercially-available finite element software to predict the locations where a wave defect is most likely to form. This model can

be used to guide materials selection (e.g., weave pattern or non-crimp fabric architecture, tow size, ends/cm), fabric placement and orientation, and local pressure and friction effects to minimize manufacturing-induced wave defects.

(b) The beam/shell model can also capture the shearing of the yarns that occurs during manufacturing, and thus can lead directly to a structural model of the cured composite blade. The "as-manufactured" model can then be subjected to static and dynamic loading conditions that can be used to predict in-use performance and to inform strain field and dynamic measurements on real structures. Any significant deviations in measured response can suggest defects and/or non-visible damage prior to failure. This ability to directly connect design to manufacturing to performance represents a valuable tool for exploring new blade materials, manufacturing process modifications, and structural designs.

(c) Location of the wave defect – both within the thickness and along the length – had the greatest effect on strength reduction. Of the other two parameters – wave amplitude and aspect ratio -- aspect ratio has the least effect. The presence of the wave defect led to strain amplification and subsequent failure.

(d) The ability of digital image correlation (DIC) to make large area measurements of strain fields and displacements has been demonstrated. This technique has shown the capability to detect wave defects on the manufacturing floor, and to detect defects and damage in full-scale blade tests and while rotating in-service. This improved, field-ready NDI and SHM technique can greatly reduce the likelihood of unexpected, catastrophic failures and thus can allow less conservative and more affordable blade designs.

(e) The materials, modeling, manufacturing, and NDI/SHM advances are applicable to other composite structures, including but not limited to aircraft, automotive, and civil structures.

(f) This project has involved 9 graduate students and 4 undergraduates, who have gained expertise in composite materials, wind turbine blade manufacturing, mechanics and modal analysis, and digital image correlation and other NDI/SHM techniques. Of these students, several have graduated and gone onto wind energy and related industry and federal lab positions. For example, Bruce LeBlanc

graduated with his MS, was hired by Sandia, and is actively working in the wind area. Eric Harvey will graduate in December with his MS and is currently working at the MassCEC/NREL Wind Technology Testing Center. Konstantine Fetfasidis completed his PhD and is currently working at a small company that develops Unmanned Aerial Vehicles. Tim Marinone held a summer intern position at LANL working on LANL's 9 meter blade, graduated with his MS, and currently works at ATA Engineering on structural dynamic testing including wind energy applications. Jen Carr will graduate with her MS in Spring 2013 and is currently doing an intership at MIT Lincoln Labs. Julie Harvie worked at LANL as a summer intern on a turbine blade project, and is starting her PhD at UML.

(g) The collaboration between NREL, Sandia, TPI, and UMass Lowell continues to strengthen with both funded projects and planned proposals. UMass Lowell hosted a Wind Energy Workshop in September 2011, sponsored in part by the National Science Foundation (NSF). Over 150 participants from industry, federal labs, and academia contributed to the presentations and discussions to help define the future directions of wind energy research. UMass Lowell is also a lead in the planned formation of an NSF Industry & University Cooperative Research Center (I/U-CRC), whose mission is to conduct research of interest to both, with major funding support and input provided by industry.

The key recommendations from this project include several avenues that are being pursued by the team:

(a) Fabrics and layup orientations that allow for greater shear deformation are less likely to result in a wave defect. Blade designers can use the combination of simple mechanical tests (e.g., trellis-frame, bending stiffness) and finite element modeling to more quickly explore new fabric constructions (anticipated as part of I/U-CRC).
(b) The beam/shell material model should be incorporated as an option for several commercial software packages (some preliminary interest expressed by software companies).

(c) Modal analysis and DIC can be used to more quickly and effectively qualify blades prior to shipping and monitor blades in-use. The team can work with blade manufacturers, system integrators, and wind farm owners to implement these techniques (current NSF grant on structural dynamics and modal analysis, also anticipated as part of I/U-CRC).

(d) New recyclable or reworkable materials that address the looming concerns about blade disposal in landfills should be explored (recent NSF grant just underway).

Acknowledgment: "This report is based upon work supported by the U. S. Department of Energy under Award No. DE-EE0001374."

Disclaimer: "Any findings, opinions, and conclusions or recommendations expressed in this report are those of the author(s) and do not necessarily reflect the views of the Department of Energy"

Table of Contents

Appendix K Impact Testing of CX-100 Wind Turbine Blades (MODAL DATA)
MACL Report # L111625 dated 16 June 2011

Appendix L Impact Testing of CX-100 Wind Turbine Blade without Saddle
SDASL Report # L111625-1 dated 17 February 2012

Appendix M Impact Testing of CX-100 Wind Turbine Blade with Saddle
SDASL Report # L111625-2 dated 17 February 2012

# 1. Introduction

## 1.1 Purpose and Scope of Report

The purpose of this final report is to communicate the key conclusions and to document the complete results of the DOE-funded project on the "Effect of Manufacturing-Induced Defects on Reliability of Composite Wind Turbine Blades. For ease of reference, the main results are summarized in the Executive Summary and Section 2. Full reports for each of the Major Efforts are provided as separate appendices that serve as stand-alone documentation for that topic. In addition, papers and reports that summarize the results contributed by various partners (e.g., Luna Innovations, NASA) are also included as appendices for completeness.

## 1.2 Personnel Involved in the Efforts

UMass Lowell

| **Personnel** | **Role/Expertise** |
|---|---|
| UMass Lowell | |
| Julie Chen | PI/ fabrics and composites, mechanical characterization, composites manufacturing |
| Chris Niezrecki | Co-PI/ digital image correlation, nondestructive inspection, structural dynamics |
| Jim Sherwood | Co-PI/ finite element modeling, fabrics and composites, mechanical characterization |
| Peter Avitabile | Co-PI/ analytical and experimental structural dynamics |
| Konstantine Fetfasidis and Siqi Wei | Graduate students/ composites and finite element modeling |
| Bruce LeBlanc and Troy Lundstrom | Graduate students/ digital image correlation and mechanical characterization |
| Javad Baqersad, Tim Marinone, Jennifer Carr, Julie Harvie, Eric Harvey | Graduate students/ modal analysis (contributors, but not funded on this project) |

| | |
|---|---|
| Cynthia Mitchell, James Soteropoulos | Undergraduate students/ composites and finite element modeling |
| TPI Composites | |
| Stephen Nolet | Director, Design Engineering/ blade manufacturing |
| Sandia National Laboratory | |
| Mark Rumsey | Wind Energy Technology Department/ fatigue testing and nondestructive testing |
| National Renewable Energy Laboratory | |
| Scott Hughes | National Wind Technology Center/ 9-meter blade testing |

## 2. Discussion of Major Efforts on Project

### 2.1 Fabric Characterization

The credibility of the finite element simulations is dependent upon an experimental characterization of the dry fabric material as well as the cured composite architecture. For the CX-100 blades, six different non-crimp fabrics (NCFs) were studied (Fig. 2.1.1).

*Figure 2.1.1 Examples of non-crimp, double bias non-crimp, and random mat fabrics*

The mechanical behavior of the NCFs was defined in terms of the in-plane shear stiffness, yarn tensile stiffness and bending stiffness, as well as the friction between contacting layers. A shear-frame test (Fig. 2.1.2) was used to characterize the in-plane shear behavior of each fabric, and uniaxial tensile tests were performed on individual yarns to quantify the tensile stiffness of the fabric yarns. The bending stiffness was characterized by hanging fabric samples

vertically and applying a horizontal load to displace the tip of the samples. The deformed profile was plotted digitally and the moment-curvature relation was determined.

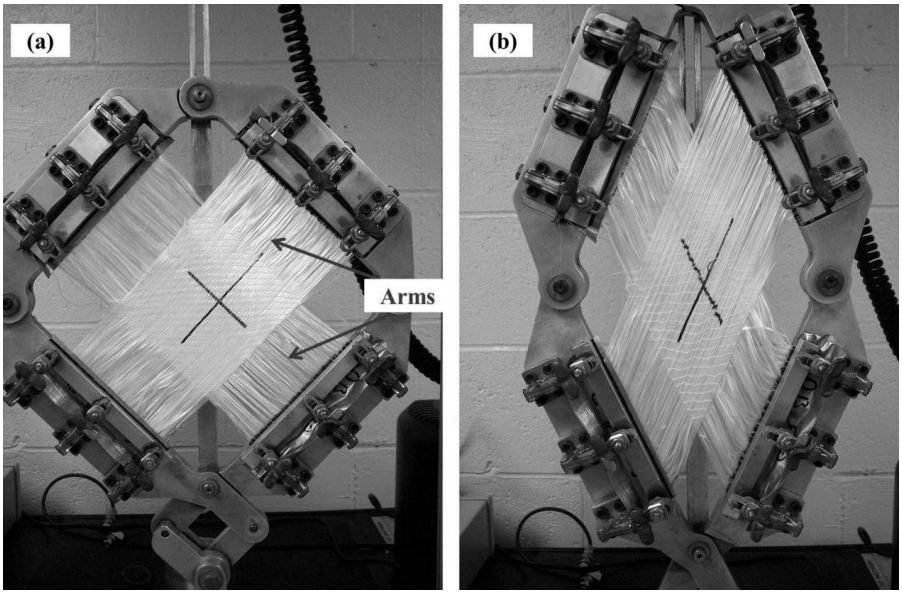


*Figure 2.1.2. Example of trellis-frame (shear frame) test (a) before deformation; (b) after shear deformation*

The differences in shear behavior of the NCFs can be seen in Figure 2.1.3. Such differences can have an effect on the formation of wave defects and general formability of the material into the mold.

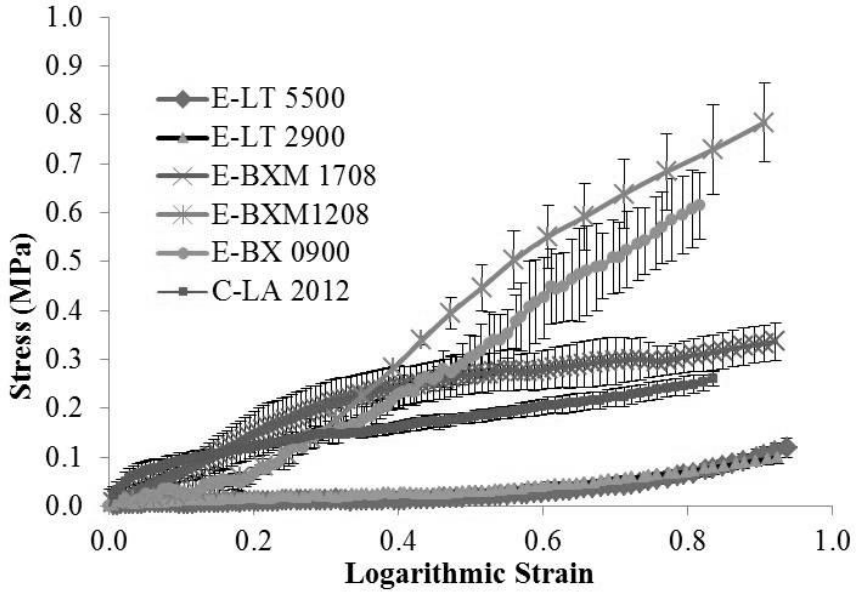


*Figure 2.1.3. Shear Response of CX-100 Non-Crimp Fabrics*

Appendix A provides more details on the materials, test setups, and results for the CX-100 fabrics for shear, tensile, and bending response. This experimental data was used as input properties to develop the beam-shell material models.

## 2.2 Simulation of the Blade Manufacturing Process

A discrete mesoscopic approach using 1-D beam and 2-D shell elements (Fig. 2.2.1) was used in the commercially available finite element software, Abaqus, to model the mechanical behavior of six different non-crimp fabrics (NCFs) used in a 9-m long wind turbine blade (CX-100) manufactured by TPI Composites in Warren, RI.

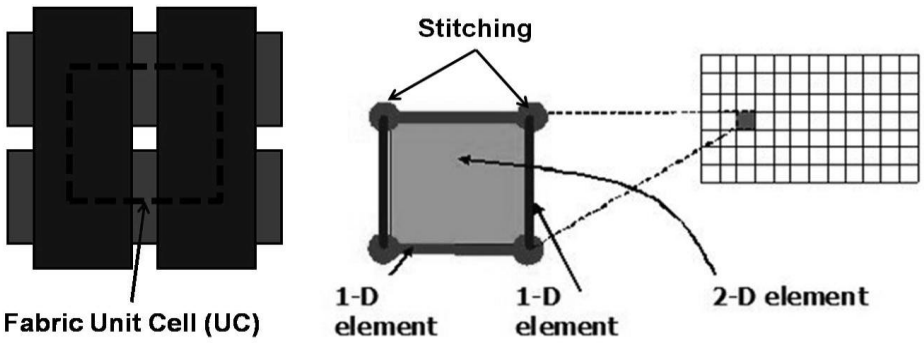


*Figure 2.2.1 Principle of the discrete mesoscopic beam/shell model for fabrics*

In the finite element model for the manufacture of the blade, the hand layup of fabric layers is simulated by using a rigid core (punch) to press the fabric into the fixed, rigid mold (2). The punch is allowed to move only in the vertical direction. Additionally, rigid binders which can translate vertically, provide in-plane tension in the fabric to prevent folding and sliding of the fabric layers as they are pressed into the mold by the punch. This forming simulation is done using the explicit formulation in Abaqus which was chosen for computing time efficiency, relatively robust contact algorithms and the option to account for the mechanical behavior of the fabrics via user-defined material models. To save computation time, layers are pressed into each mold in groups. After initially being pressed into the mold using the rigid punch, additional pressures are subsequently applied to press the layers tightly into each mold.

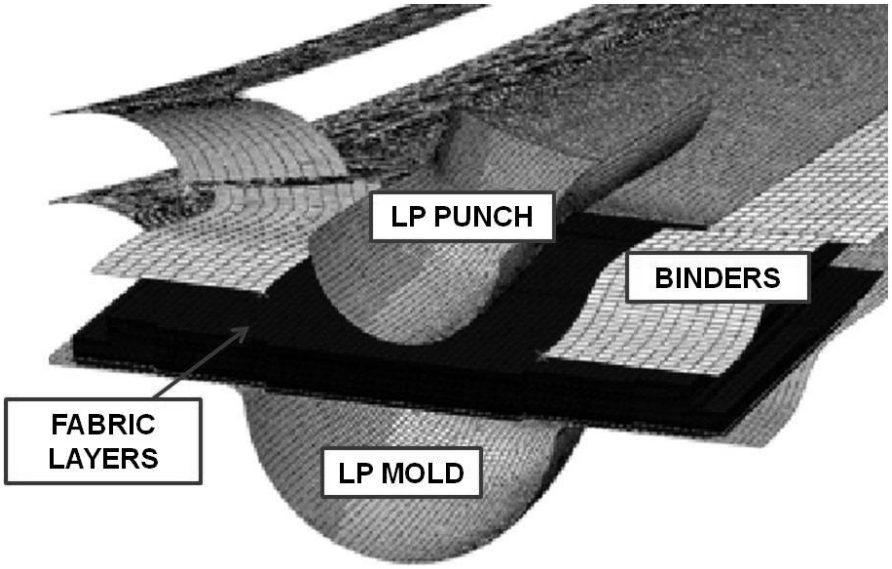


*Figure 2.2.2. Punch pressing fabric layers into the LP mold. Binders are used to provide in-plane tension in the fabric*

After all of the layers of fabric have been pressed into the molds, the compaction of the fabric layers is simulated by applying a pressure equivalent to atmospheric pressure directly onto the surface of the top layers. It is during this stage in the manufacturing process that fabric layers may bunch together to form out-of-plane wave defects that eventually compromise the performance and reliability of wind turbine blades. Because the formation of wave defects most likely occurs during the hand layup and vacuum compaction stages of the manufacturing process, the resin infusion process is not simulated in this research. Instead, it is assumed that once the layers of fabric have been placed in the molds, the resin is evenly distributed across each mold with a fiber volume fraction of 55%, which is typical for the CX-100 blades manufactured using the SCRIMP® process. After the LP and HP molds are individually modeled, they are bonded together with tie constraints, resulting in the full CX-100 blade model.

Simulations were performed to mimic the hand-layup of the several plies during the manufacturing process. Upon inspection of the deformed layers, none of the fabrics experienced excessive in-plane shearing to conform to the molds of the blade, but some small in-plane waviness was observed. Figure 2.2.3 illustrates the effect of the different fabric architectures on the deformation behavior of the fabric as a result of compaction. Similarly, the yarns of the fabric layers were shown to be below the tensile load breaking threshold. After all of the layers were pressed into the low-pressure and high-pressure molds of the wind turbine blade, a pressure

equivalent to atmospheric pressure was applied onto the top-fabric surfaces to simulate the vacuum compaction stage of the manufacturing process. During this stage in the process, it was shown that the bending stiffness of the material as well as the friction between layers and the location of ply drops were parameters that could influence the formation of out-of-plane wave defects. However, when representing the actual CX-100 design, the simulation confirmed that the design was not vulnerable to manufacturing-induced wave defects.

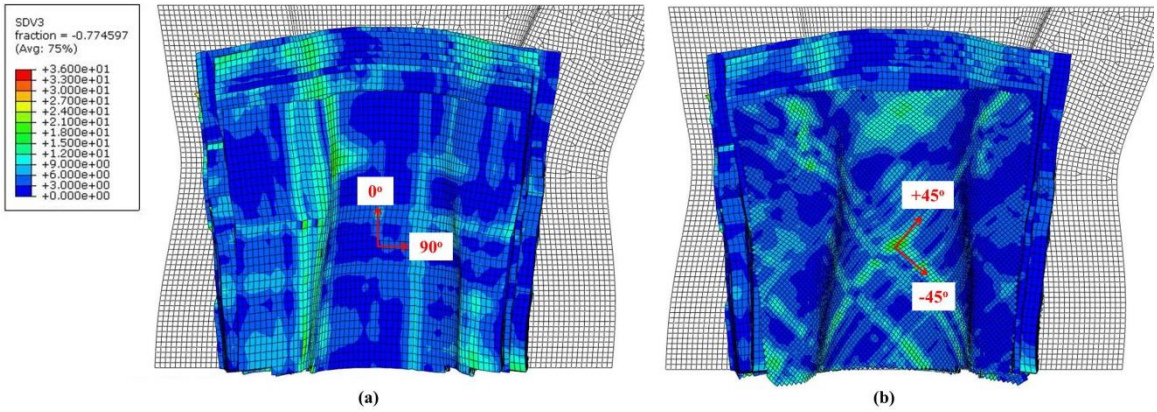


*Figure 2.2.3. In-plane shear angle contours for (a) 0/90 biaxial NCF and (b) +/-45 double bias NCF*

The model should be capable of capturing the deformation of the yarns during fabric layup (by hand or automated layup) as well as during the vacuum compaction stage of the manufacturing process, thus giving insight as to areas where defects may be developed. Subsequently, by knowing how the yarns have deformed during these two stages, the structural stiffness of the blade can be predicted with fewer assumptions and without knockdown factors, thereby linking the resulting composite structure to the manufacturing process. These structural models can then predict the effect of defects on various blade sizes and in different locations within the blade. This simulation of the manufacturing process and subsequent structural stiffness can help guide design decisions such as the number of layers and orientations required for a given selection of fabric(s) that will reduce weight while maximizing structural performance.

## 2.3 Effects of Wave Defects

Wave defects with controlled dimensions were embedded in three different locations along the spar cap of a CX-100 blade (Table 2.3.1, Figure 2.3.1). The blade was fixed at the root and loaded at the 6.75-m location with a 2.3-kN weight.

**Table 2.3.1. Dimensions and locations of wave defects embedded in CX-100 spar cap**

| Defect amplitude (mm) | Defect aspect ratio (Length/Amplitude) | Distance from blade root (m) |
|---|---|---|
| 3 | 5 | 6.0 |
| 3 | 10 | 5.0 |
| 3 | 15 | 3.5 |


*Figure 2.3.1 Insertion of wave defects (a) on top of double-bias layers and (b) beneath the first spar-cap layer in CX-100*

Figure 2.3.2 shows an example of a digital image correlation (DIC) measurement at the 5.0-m location along the low pressure (LP) side of the CX-100. The strain across the surface of the blade as indicated by the double-arrow line in Figure 2.3.2 is plotted in Figure 2.3.3 where the nominal strain away from the defect is compared to the magnitude of the amplified strain at the location of the defect.

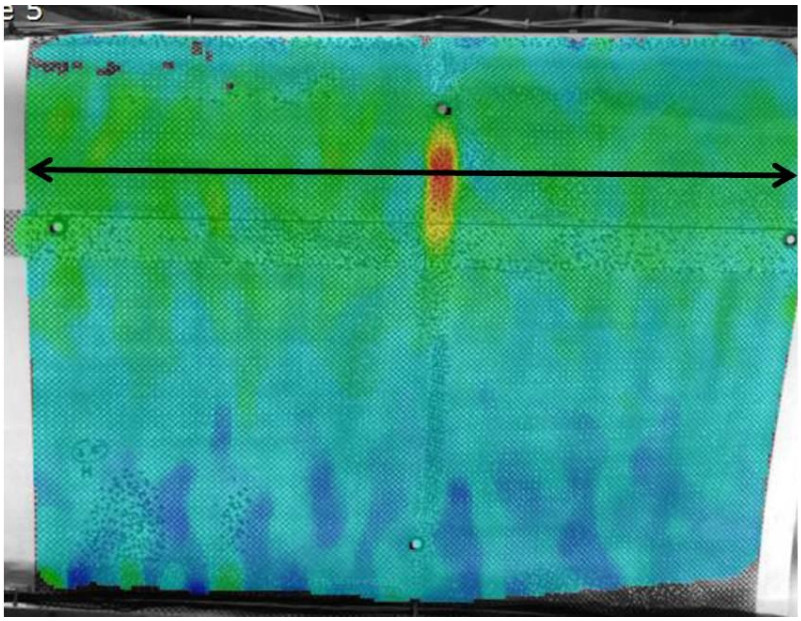

*Figure 2.3.2 DIC measurement of strain at the 5.0-m location along the LP side of a CX-100 blade*

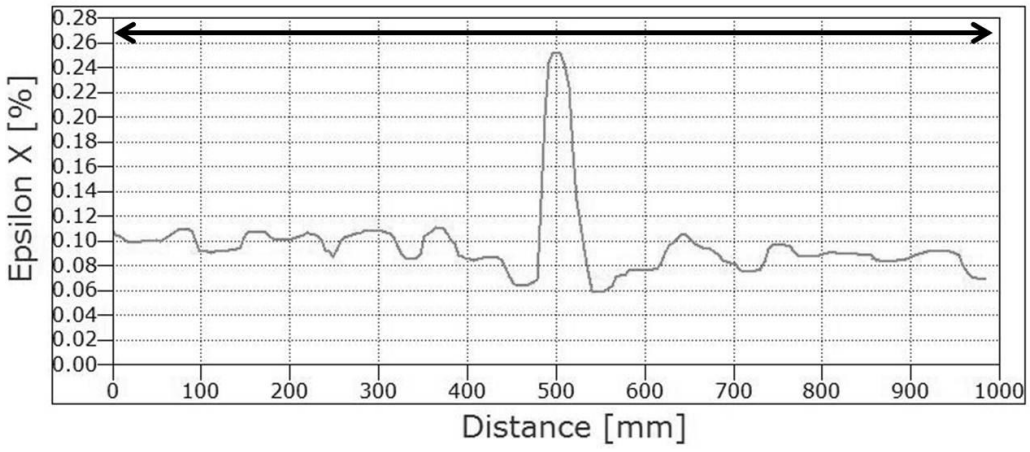


*Figure 2.3.3. DIC strain measurements along a line of interest passing through the location of a defect*

As was done with DIC measurements in Figures 2.3.2 and 2.3.3, a double-arrow line of interest can be drawn across the LP surface of the finite element model of the blade (Figure 2.3.4) to compare the magnitude of the nominal strain away from the defect to the magnitude of the amplified strain at the location of the defect (Figure 2.3.5).

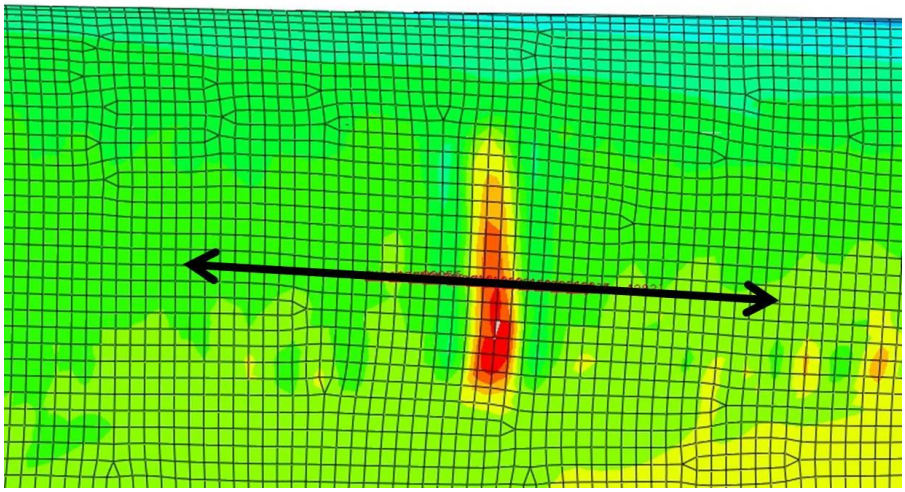

*Figure 2.3.4. Finite element model results: Line of interest across the LP blade surface to compare nominal and amplified strain at defect location*

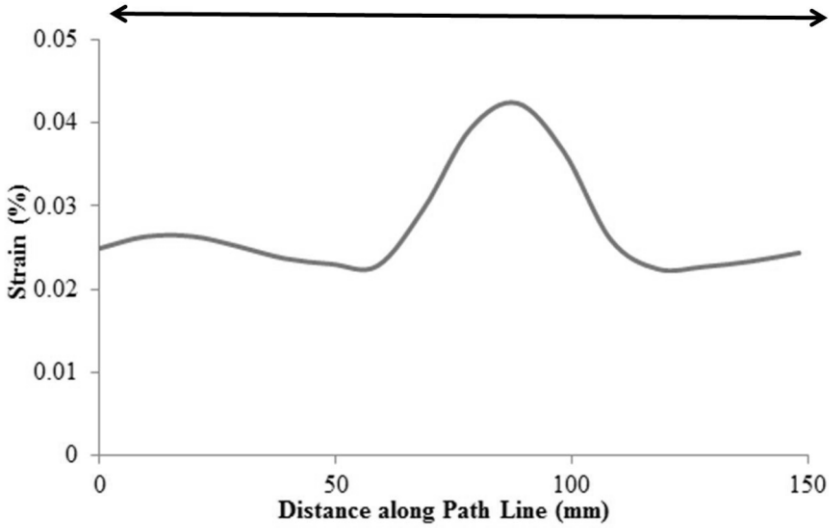


*Figure 2.3.5. Finite element model results: Strain along the line of interest drawn at the location of a wave defect in the blade*

Despite using only the structural properties of an E-LT 5500 laminate, the finite element model showed the amplification of strain at the location of the three defects. This amplified strain was similar to typical measurements made using a digital image correlation system, providing support for the validity of the model.

## 2.4 Coupon Testing

To understand the defect parameters of significance, glass-fiber/epoxy coupons were fabricated with wave defects and subsequently tested to measure the reduction in compressive strength and fatigue life relative to wave-defect-free coupons as a result of wave defect through-thickness location, wave amplitude, and wave aspect ratio (wave length/wave amplitude) (Figure 2.4.1).

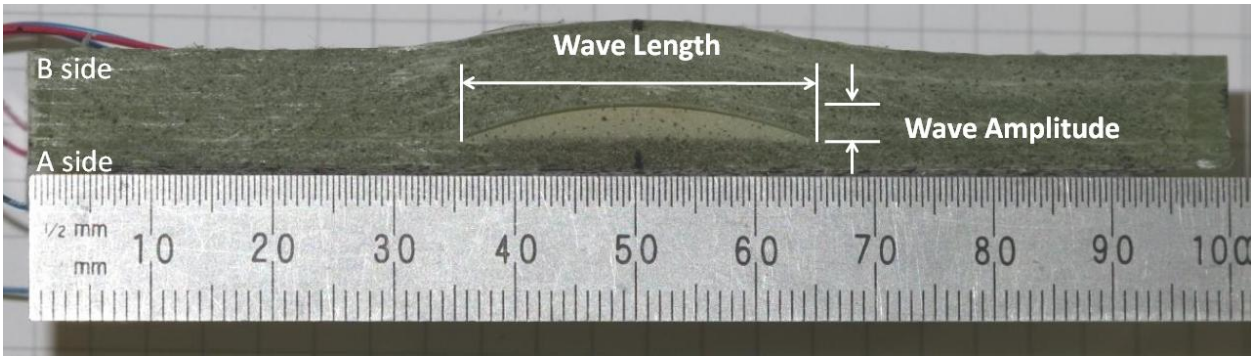


*Figure 2.4.1 Example of coupon with wave defect dimensions.*

Pre-cured epoxy-only wave defects with controlled dimensions were inserted into various coupon samples. Additionally, a nine-meter turbine blade was manufactured with pre-cured, controlled wave defects in prescribed locations along the spar cap and then cut into test coupons. The subsequent sections of Appendix D describe the coupon fabrication process, experimental parameters, and the results of the static and fatigue tests.

Figure 2.4.2 shows an example of a static compression test setup. The effect of aspect ratio and through-thickness location is shown in Figure 2.4.3. From these results, it is clear that the effect of location is more significant that the difference between aspect ratios of 5, 10, and 15.

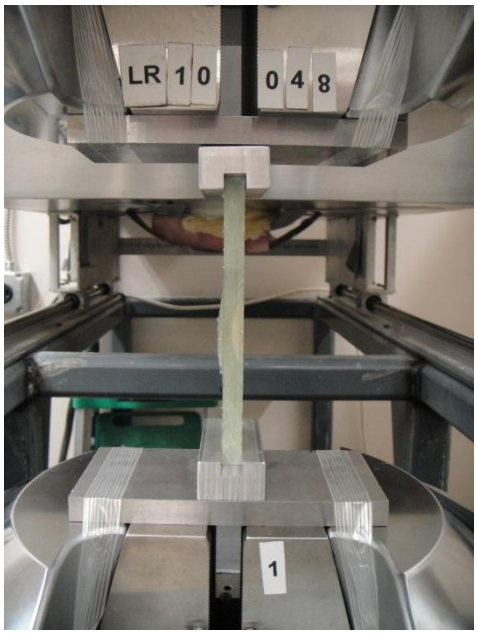


*Figure 2.4.2 Typical static compression test setup*

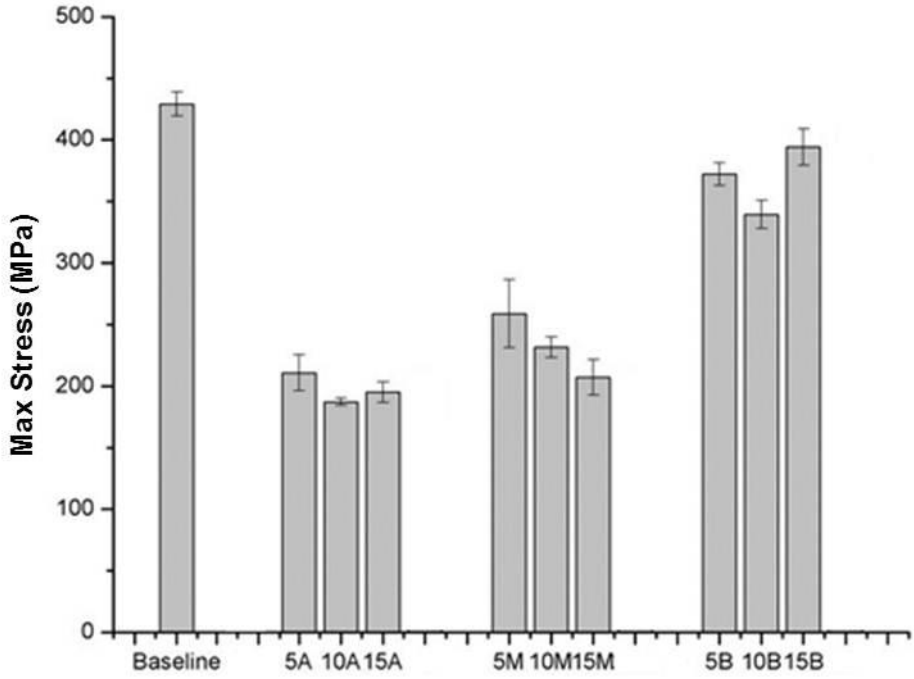


*Figure. 2.4.3. Effect of aspect ratio and through-thickness location on compressive strength of test coupons*

Three-dimensional Digital Image Correlation (3D DIC) measurements and finite element (FE) models were used for data comparison and interpretation purposes (Figure 2.4.4). As the

amplitude of the embedded wave defect increased, the level of strain amplification visibly increased on the surface near the defect, indicating that perhaps the wave amplitude is a more critical defect parameter in terms of compressive strength than the aspect ratio.

| 1 mm | 2 mm | 3 mm |
|---|---|---|
| 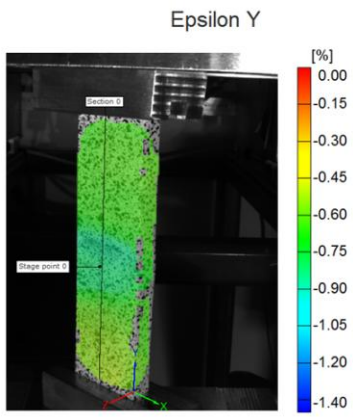 | 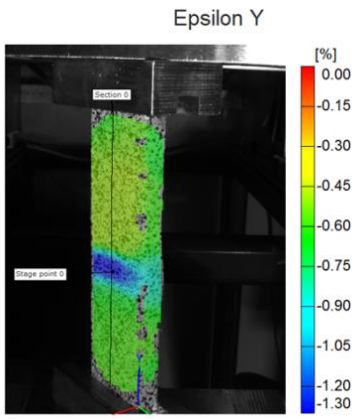 | 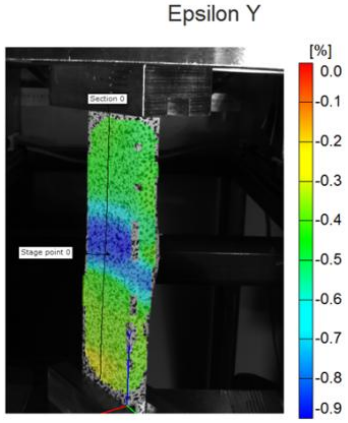 |



*Figure 2.4.4. Examples of DIC strain measurements during compression tests with aspect ratio of 10, but differing wave amplitudes.*

Fatigue tests were also conducted on the coupons. Figure 2.4.5 illustrates a typical failure for a fatigue specimen subjected to increasing load levels.

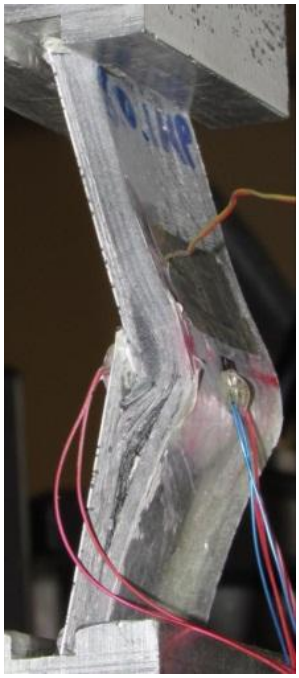

*Figure 2.4.5. Typical failure mode during fatigue test.*

The results of this study provide insight on the impact of wave defects on the structural integrity, as observed in the associated strain amplification in the region surrounding the defect, of composite wind turbine blades and other structures made using a similar manufacturing process.

## 2.5 Digital Image Correlation Effects

Digital Image Correlation (DIC) measurements were made on three separate TPI Composites CX-100, 9-meter, wind turbine blades (Sandia "Sensor Blade", LANL Blade and UMass Lowell Defect Blade). Figure 2.5.1 shows the LANL blade with the DIC patterning on the surface.

*Figure 2.5.1 LANL defect-free blade test setup at NREL with DIC patterning.*

For the UMass Lowell defect blade, the DIC was able to clearly show the location of the defect. As the blade was cycled, the strain amplification in the vicinity of the defect became

even more apparent as is shown in Figure 2.5.2 for the 5m high pressure side, defect location (area where failure first occurred).

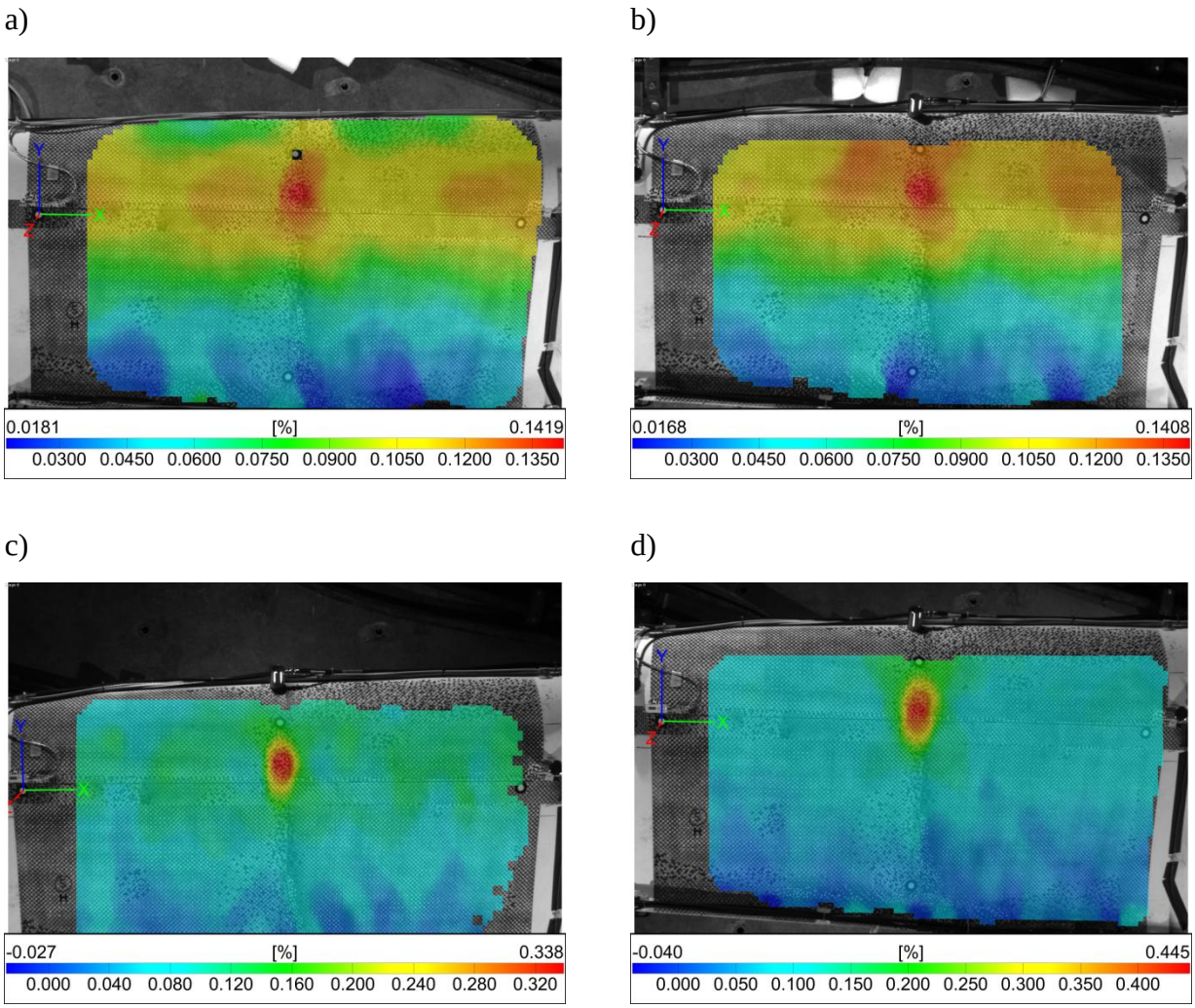


*Figure 2.5.2. Strain contour plots for the 5.0-meter section at a) 0 cycles; b) 25,603 cycles; c) 755,049 cycles; d) 1,803,350 cycles.*

The results of the tests on the Sandia blade revealed that DIC could readily identify changes in strain and surface geometry due to cracks present in the blade after being subjected to fatigue failure. The Sandia blade tests also revealed that multiple images can be stitched together to obtain the blade geometry, deformation, and full-field strain over the entire blade area. The LANL blade served as a baseline (defect-free blade) for comparison in which DIC was used to interrogate the same six areas that possessed defects in the UMass Lowell blade. The results revealed that there was no significant increase in strain at these locations in the defect-free blade. DIC was also used to interrogate the six different locations that possessed defects in the UMass

Lowell blade. The results indicate that DIC can be used as a full-field inspection technique to identify defects (via strain amplification) and monitor the progression of crack growth or structural changes. The primary results are summarized in Appendix E.

### 2.6 Full-Blade Testing and NDI/SHM (acoustic emission, fiber optic sensors, PZT sensors)

The report in Appendix F from NREL describes the laboratory fatigue testing of the UML Defect 9-m wind turbine blade conducted at the National Wind Technology Center (NWTC) in Colorado. The test was performed with the blade cantilevered to the 1,360-kN-m yellow test stand (Figure 2.6.1). Unique to this blade were manufactured wave defects that were fabricated in the spar cap laminates at the 3.5-m, 5-m, and 6-m stations, on both the high pressure (HP) and low pressure (LP) sides. An accelerated 1-million cycle design life fatigue load was applied to the blade before increasing loads in discrete steps up to 130% of the target fatigue loads, at which point a 2.5-cm long crack was observed at the 5-m station on the HP surface spar cap, biased towards the leading edge (LE). (Figure 2.6.2) The test ran for approximately 1.9-million cycles before the failure. After the fatigue test was concluded, a single-point quasi-static load to failure was conducted to obtain additional information about the residual strength of the inboard wave defects located at the 3.5-m station.

*Figure 2.6.1 NREL flapwise fatigue test setup for 9-meter UMass Lowell defect blade.*

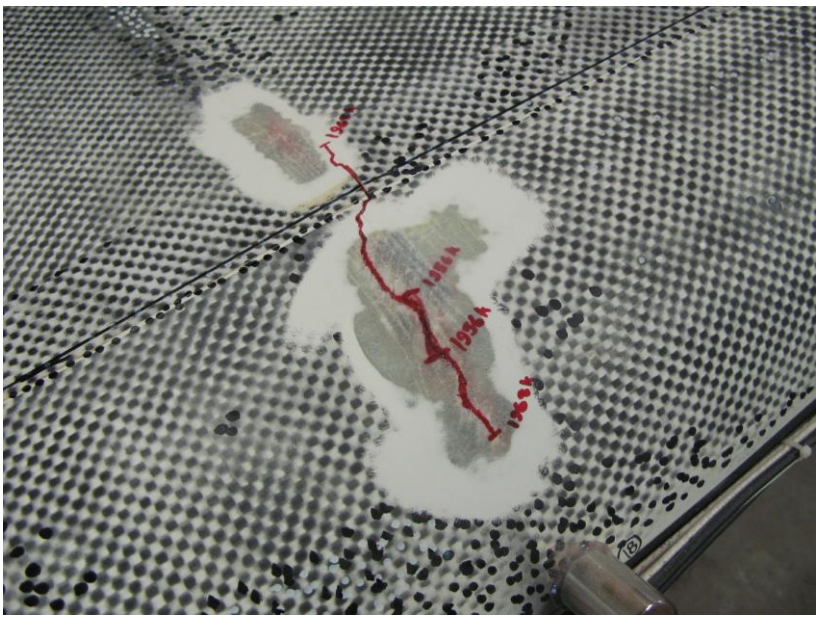

*Figure 2.6.2 Structural failure near wave defect at 5m location, after approximately 1.9million cycles at increasing load levels.*

Several nondestructive evaluation (NDE)/structural health monitoring techniques were utilized on the blade. Both the Luna Innovations fiber optic sensors and the UML digital image correlation measurements reported that there were stress risers on the order of 2-3 times in the

defect areas as compared to surrounding areas, as shown in Figure 2.6.3. The results from the foil strain gages correlated well with the fiber optic measurements at the same location, but the foil gages, positioned half a meter away from the defects, were not able to capture the strain amplification due to the defect.

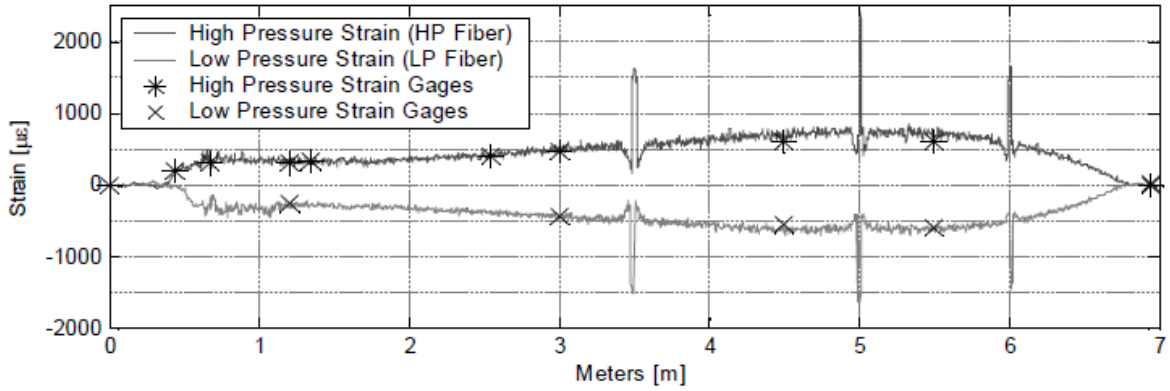


*Figure 2.6.3 – Fiber Optic and Foil Strain Gage Measurement Comparison (figure courtesy Luna Innovations Inc.)*

In addition to the Luna sensors, both acoustic emission sensors (Sandia) and PZT sensors (NASA Kennedy Space Center) were utilized during the NREL fatigue testing. Results of these studies are included in Appendices G and J.

## 2.7 Modal Analysis and Impact Testing

Modal studies were conducted at two distinct times – (a) before the manufactured blade left TPI; and (b) at the initial NREL test setup for the blade. The main focus of the former was directed toward the identification of mode shapes for two TPI-fabricated, UMass Lowell CX-100 wind turbine blades to allow for comparison and examination of variability between blades.

Figure 2.7.1 shows the UMass Lowell defect blade being tested at TPI with accelerometers attached. The blade was tested in a free-free condition and was impacted with a calibrated impact hammer. Five (5) tri-axial accelerometers were attached to the high pressure side of the blade.

*Figure 2.7.1 Free-free modal test setup for 9-m UMass Lowell defect blade at TPI.*

Table 3.1 shows the results of the comparison between the two UMass Lowell defect blades fabricated by TPI. These results suggest that the modal responses of the two blades are similar and thus the relatively small structural variability is acceptable.

Table 3.1: Comparison of Results between Cut-Up and Uncut-Up Blades

| Pair # | Cut-Up | Uncut-Up | % Difference | MAC | Mode Description |
|---|---|---|---|---|---|
| 1 | 7.90 | 7.76 | 1.80 | 98.3 | 1st Flapwise Bending |
| 2 | 15.97 | 15.67 | 1.89 | 96.2 | 1st Lag Bending |
| 3 | 20.84 | 21.26 | -1.94 | 97.6 | 2nd Flapwise Bending |
| 4 | 32.45 | 31.34 | 3.55 | 95.9 | 3rd Flapwise Bending |
| 5 | 43.20 | 43.60 | -0.90 | 73.3 | 2nd Lag Bending |
| 6 | 50.87 | 49.68 | 2.40 | 96.0 | 4th Flapwise Bending |
| 7 | 65.55 | 63.09 | 3.90 | 80.8 | 1st Torsion |
| 8 | 70.45 | 68.23 | 3.26 | 90.2 | 3rd Lag Bending |

At NREL, measurements were taken on the UMass Lowell blade while clamped in the test fixture, both without and with the support saddle (Figure 2.7.2)

*Figure 2.7.2. 9-m UMass Lowell defect blade clamped (a) without, and (b) with the saddle at NREL*

Figure 2.7.3 is a schematic of the blade, showing the locations of the impacts and the accelerometers. Table 2.7.2 summarizes the measurement frequencies and modes for the blade with the saddle attached. More detailed discussion of the theory, the mode shapes, and the results from each test are provided in Appendices K, L, and M.

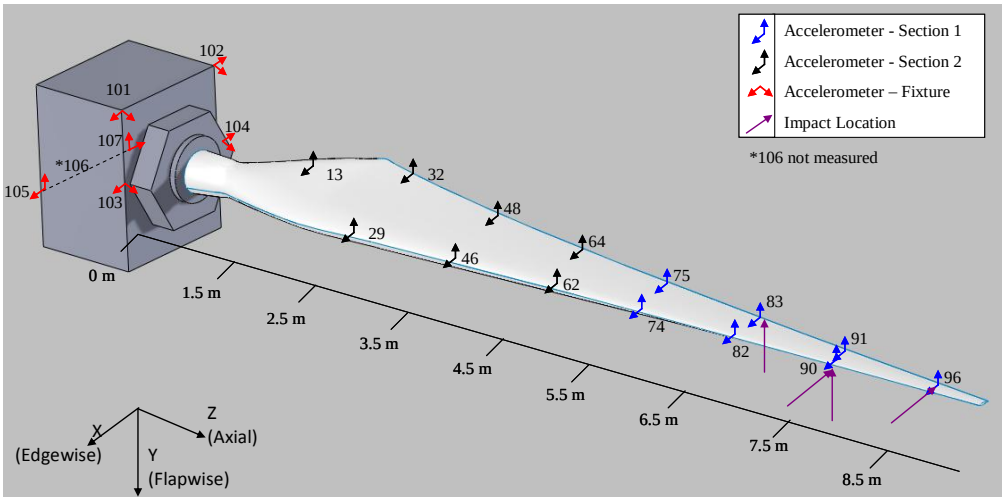


*Figure 2.7.3. Schematic showing impact locations and accelerometer locations for modal analysis of UMass Lowell defect blade in test stand at NREL.*

*Table 2.7.2. Fixed-Free CX-100 Frequencies and Modes with Saddle*

| Mode | Frequency (Hz) | Damping | Description |
|---|---|---|---|
| 1 | 1.868 | 0.28% | Flap |
| 2 | 2.728 | 0.24% | Edge |
| 3 | 8.886 | 1.40% | Flap |
| 4 | 9.671 | 0.43% | Flap |
| 5 | 16.722 | 0.68% | Flap |
| 6 | 22.971 | 1.95% | Flap |
| 7 | 25.258 | 3.44% | Edge |
| 8 | 33.764 | 0.61% | Edge |

## 3.0 Summary

This Executive Summary is meant to provide a brief overview of the key activities and outcomes of this DOE project. A more complete description of the materials, manufacturing methods, experimental setups, the model generation, and the measurement techniques is provided in the Appendices. Each Appendix also discusses in greater detail the results from the many experimental and modeling cases conducted as part of this work. The Appendices from our partners are provided (with their permission) to give a more comprehensive sense of the breadth of knowledge gained from this effort, as well as the integration of the multiple components – e.g., materials characterization, finite element modeling, blade testing, sensor measurements. This project has advanced not only our understanding of approaches to minimize wave defect formation, reduce their detrimental impact, and detect them earlier, but the project also has contributed to practical methods and tools that can be used by industry to improve the design, manufacturing process, and nondestructive inspection/structural health monitoring of composite wind turbine blades.